INFRARED CCD DEVELOPMENTS: DEVICES AND APPLICATIONS

B R Holeman*

1 INTRODUCTION

For many applications single and multi-element infrared detectors can now be made which closely approach the performance set by the statistics of the incident flux. At first sight there is no point in further development of detectors. This paper will outline these performance limits and describe the logic behind the major gains to be expected from infrared detectors with signal processing on the focal plane. The main families of sophisticated detector types will be reviewed and examples of the current state-of-the-art described.

2 CONVENTIONAL DETECTORS

(a) Photon Detectors

For ideal photon detectors the detector response is proportional to the total detected photon flux out to a given long wavelength (ie low energy) limit, so that, if this photon flux is ϕ, then the signal-to-noise ratio is

$$SNR = \frac{eA\phi}{(2e\ A\phi\Delta f)^{\frac{1}{2}}} = \left(\frac{eA\phi}{2\Delta f}\right)^{\frac{1}{2}}$$

where
- ϕ is photon flux in photons $cm^{-2} sec^{-1}$
- A is detector area cm^2
- Δf is the electronic bandwidth Hz
- e is the electronic charge.

For a photon detector that closely approaches the performance of an ideal detector, the SNR will not be further degraded and the usual area and bandwidth independent figure of merit D* can be defined. The monochromatic D^*_λ for a signal of wavelength λ, broadband background, at the detector peak wavelength λ is

$$D^*_\lambda = \frac{\lambda}{hc} \frac{1}{(2\int_o^\lambda N_{bb} d\lambda)^{0.5}} = \frac{1}{h\nu(2\phi)^{0.5}}$$

D^*_λ and D^* are usually quoted for a small signal (monochromatic or 500K black body respectively) superimposed on a larger background flux of specified temperature, usually ambient.

The main impetus for infrared photon detector development has for many years been terrestrial thermal imaging. Systems must detect the small changes in photon flux due to temperature or emissivity changes in objects near ambient temperature. A somewhat simpler task is the detection of objects at temperatures well above ambient, for example heat seeking missiles.

*Royal Signals and Radar Establishment, Malvern, UK.

Fig 1 shows how some of the relevant parameters vary with wavelength. The dashed curves represent a 300K black body source with no atmospheric attenuation, while the solid curves allow for a specified atmosphere and a typical path length. The curves labelled 'Flux' give the integrated flux up to the wavelength plotted, while those labelled 'Flux spectrum' give the spectral dependence. There are three main points to note. The 3-5μm waveband is split into two components centred at 3.7 and 4.5μm respectively while the 8-13μm waveband is nearly continuous. The integrated flux in the 8-13μm waveband is about two orders of magnitude greater than for the 3-5μm waveband. Finally, the absolute flux in the 8-13μm waveband is very high. A zenith sun incident on a pure white reflector produces a visible photon flux of 10^{21} to 10^{22} photons m^{-2} sec^{-1}, of the same order as the 8-13μm 300K flux.

The thermal imager must, however, detect flux changes and not total flux. The flux change with temperature is about 3% K^{-1} and 1.5% K^{-1} in the 3-5 and 8-13μm wavebands respectively. In order to compare system performance for terrestrial thermal imaging a figure of merit M^*[1] has been defined. This takes into account the atmospheric transmission and the variation of contrast with wavelength to give a waveband independent figure of merit M^* given by

$$M^* = \frac{\int_o^{\lambda_c} \tau_\lambda \eta_\lambda \frac{\partial N_{bb_\lambda}}{\partial T} d\lambda}{\left(2 \int_o^{\lambda_c} \eta_\lambda N_{bb} d\lambda\right)^{\frac{1}{2}}}$$

where the integration is carried out to the cut-off wavelength, λ_c, of the detector.

Fig 2 shows D^*_λ and M^* versus cut-off wavelength, λ_c, for an ideal photon detector (ie one with $\eta_\lambda = 1$ for $\lambda = 0$ to λ_c, and $\eta_\lambda = 0$ for $\lambda > \lambda_c$). The effects of the split 3-5μm waveband and the atmospheric absorption between the 3-5 and 8-13μm wavebands are clearly demonstrated. Only two particular path lengths have been selected, for a full analysis the values of M^* must be calculated for the various atmospheric conditions and ranges of interest.

For many applications in thermal imaging the detectors closely approach the limits set by the incident photon flux, and further performance improvements are only possible if a greater flux is detected. A simple single detector scanned in a standard TV format uses roughly 0.001% of the available photons. Performance is improved by adding extra detectors in ways which will be described in section 4. In general, if this is done with no loss in theoretical performance, the signal will increase as the number of detectors, and the noise as only the square root of this number. For an array of N detectors each with given D^* and M^* (either monochromatic or black body), the effective values become $D^*N^{\frac{1}{2}}$ and $M^*N^{\frac{1}{2}}$ respectively. It is important to realize that signal processing must be of adequately low noise, and the whole array should remain background limited for optimum performance.

As the ratio of M^*_{3-5} to M^*_{8-13} is about 6 in favour of the 8-13μm waveband, an ideal array requires about 36 times as many detectors in the 3-5μm waveband as an equivalent array in the 8-13μm waveband, again for terrestrial thermal imaging.

The state-of-the-art of photon detectors has been reviewed by several authors recently[2],[3]. Table 1 summarises the current state-of-the-art of photon detectors. Extrinsic silicon requires cooling below 77K (to 25K for gallium doped silicon for 8-13μm, and to 40 to 60K for indium doped silicon for 3-5μm). However at these temperatures very good performance is obtained and detectors remain background limited in very low photon fluxes. At 77K both $Cd_xHg_{1-x}Te$(CMT) and $Pb_xSn_{1-x}Te$(LTT) can give very good performance in both wavebands, for instance CMT can remain background limited at only 8^o field of view. At the next operational temperature of interest, thermoelectric cooling to 180-200K, performance is markedly reduced with no background limited detectors for 8-13μm, and relatively small gains being possible with decreasing field of view for 3-5μm.

TEMPERATURE OF OPERATION	SUB 77K	77K	180-200K
Background limited in less than 2πFOV	Extrinsic silicon In (3-5) Extrinsic silicon Ga (8-13)	CMT (3-5) CMT (8-13) LTT (8-13) LTS (8-13) PbSe (3-5) InSb (3-5)	
Not background limited in less than 2πFOV			CMT (3-5) CMT (8-13)

TABLE 1 Performance of current photon detectors against 300K background
LTS = $Pb_xSn_{1-x}Se$. 3-5 and 8-13 refer to waveband of operation

In use in a thermal imager the detector must have a high quantum efficiency (to maximise D* and M*) and must therefore generate an output with a large offset due to the background photon flux. The problem of detecting temperature variations of 0.1^oC at normal ambients corresponds to contrasts of only 0.3 and 0.15% in the two wavebands. This should be compared with imaging at visible wavelengths where contrasts less than a few per cent are not detectable by the eye.

(b) Bolometric detectors

While a range of bolometric detectors exist (for example Golay cell, thermopiles and superconducting bolometers) the only bolometer of real concern to us here is the pyroelectric bolometer. An ideal bolometer has an equal energy response to all wavelengths so that D* is essentially independent of wavelength.

A background limit can be defined for bolometric detectors, giving

$$D^* = \frac{1}{(16\sigma k\, T^5)^{0.5}}$$

where σ is Stephan's constant, k is Boltzmann's constant, T is the temperature of detector and background, and unit emissivity of detector and background is assumed. For T = 300K, $D^* = 1.8.10^{10}$. The theoretical value of D* is increased only marginally by cooling the detector.

In practice the pyroelectric detector does not closely approach the background limit, falling short by a factor of 50 to 100 with typical D* values of 10^9 at low frequencies. The dominant materials are Triglycine Sulphate (TGS) and its derivatives, and ceramics such as Lead Zirconate-Titanate (PZT). In both cases the detector behaves like a capacitor with a parallel current generator proportional to the rate of change of temperature. For TGS the ferroelectric Curie point is 49°C and is uncomfortably low for practical applications. Derivatives of TGS have higher Curie points, and in addition can have a built-in crystal assymetry so that repoling is not required if the Curie point is exceeded.

3 IMAGER REQUIREMENTS

The simplest imager, Fig 3(a), consists of a single detector with a scanning system to produce a raster scan. For a linescan or 'pushbroom' type of system the motion of scanner or of target can produce the scan in one direction, but for two dimensional scanning both scans are required. As previously stated the $M*N^{\frac{1}{2}}$ is limited and this system is only suitable for non-critical use, or where data rates can be slow.

Detectors can be grouped to increase $M*N^{\frac{1}{2}}$ in a number of ways. In parallel scan a linear array parallel to the scan direction, fig 3(b), scans many lines at once. It may be used in a 'banded'scan, ie the array is scanned in a number of sweeps, each sweep contiguous with the preceding one, to complete one frame. The $M*N^{\frac{1}{2}}$ value is then set by the maximum number of detectors that can be fabricated, packaged and electrically handled in a dewar. Examples are 180 elements in the US common module system[4] and 192 elements constructed by Mullard[5]. This is near the practical limit of number of detectors with each one connected to a separate external amplifier.

An alternative is to use serial scan as in fig 3(c). Again each detector is connected to an external processor, but in this case this is a time delay and integrate circuit (TDI). The array is scanned in the same way as a single element detector so that every detector views every part of the image unlike the case for parallel scan. The main advantage of this is that detector responsivity variations are then cancelled out, easing subsequent signal processing for the low contrast image. As a given image point moves down the array, the signals from successive detectors are added in the shift register and a signal N times that for a single detector appears at the shift register output. As noise increases only as $N^{\frac{1}{2}}$ the expected gain in SNR of $N^{\frac{1}{2}}$ is obtained.

In practice simple serial scan is not deployed and serial/parallel scan fig 3(d), is used instead. This is a number of serial arrays each with its own shift register. The main advantage is the reduction in scan speed to values intermediate between simple parallel and simple serial scan. Most of the uniformity advantages of serial scan are obtained with fewer output channels to adjust than the case for parallel scan. A number of arrays of this type have been constructed, for example a 6 x 8 array in CMT by Mullard[5] and a 2 x 16 array in LTT by Plessey[6]. However the number of detectors in an essentially single element technology is again, as in parallel scan, limited to the order of 100 by the problem of getting leads out of the dewar.

The last system fig 3(e) is not realisable in any worthwhile form in single element, external to dewar processing. A 100 element array is only 10 x 10, most requirements call for effectively 100 x 100 and upwards.

In the visible waveband single element technology for more than a few detectors is not deployed, instead some form of multiplexing is used. This applies whether the device is electron beam read (vidicon and its variants) or all solid state (CCD, CID, X-Y addressed imagers). In order to extend this approach into the infrared, and at the same time dispense with the large number of leads needed in the dewar, it is necessary to incorporate either or both of TDI and multiplexing on the focal plane, ie at the bottom of the dewar. This now requires a vast increase in the complexity of the focal plane.

The requirements set by the imager applications can be summarised as (1) TDI and/or multiplexing at the bottom of the dewar, (2) circuit operation at cryogenic temperatures, (3) detector performance must not be degraded compared with out of dewar signal processing, (4) effective electrical and mechanical coupling of detector and signal processor and (4) very low power dissipation.

When considering the overall performance it is particularly important to remember that signal levels can be high, and that the signal to noise ratio is set by the quantum statistics. A flux of 10^{21} photons m^{-2} sec^{-1} on a detector 50 x 50μm^2 with an integration time of 1 ms and with unit quantum efficiency corresponds to $2.5.10^{10}$ electrons. This should be compared with typical silicon CCD storage wells of 10^5 to 10^7 electrons. Any process used to reduce this large signal level, for example by continuously or sequentially subtracting a fixed charge from the integrating charge so that the 'real' signal of 10^5 to 10^6 electrons remains, must not itself introduce additional noise.

The requirements set out in this section are heavily biased towards terrestrial thermal imaging. This is currently the main driving force towards detector development, and has well specified levels of photon flux, wavelength range and contrasts of interest. The main alternative area of investigation is in space applications where the atmosphere is no longer a limitation and the photon flux can now vary over many orders of magnitude depending on whether the earth is in the field of view.

4 FOCAL PLANE ARRAYS

CCD and CID technology is attractive for the signal processing requirements of focal plane arrays. Of the requirements listed in section 3, the CCD and the CID can perform the multiplex function, and the CCD can also perform the TDI function. Both technologies are low power dissipation, and can operate at cryogenic temperatures. On the debit side normal device grade silicon is insensitive to wavelengths longer than 1.1μm. The problem of making infrared focal plane arrays is that of combining the CCD/CID functions with a high performance infrared sensitive detector element.

Table 2 lists the main options. In hybrid technology, an array of detectors in a conventional infrared detector material such as CMT or InSb is linked mechanically and electrically to a conventional silicon CCD for multiplexing of TDI. In monolothic technology the CCD or CID is constructed from the infrared detector material, and CCD/CID technology is then required in materials such as InSb or CMT. Two variants retain silicon technology, the use of Schottky barriers with internal photoemission, and impurity photoconductivity in extrinsic silicon.

MONOLITHIC		HYBRID	
Intrinsic:	InSb CCD or CID	Si to	CMT
	CMT CCD		PbS
	Si Schottky Barrier		Pyroelectric
Extrinsic:	Si : In		LTT
	Si : Ga		$InAs_xSb_{1-x}$
			InSb CID

TABLE 2 OPTIONS FOR FOCAL PLANE ARRAYS

In all cases except monolithic technology in CMT or InSb the device operation differs markedly from the operation of a visible waveband imager. In the latter photon absorption creates electron-hole pairs and the charge stored is minority charge. In the case of Schottky barrier and extrinsic silicon the charge sign is that for the majority carrier, and for indirect operation the signal is fed in through a metallic interconnect. Various schemes have been proposed and fabricated to achieve efficient transfer of charge from the detector into the CCD/CID, all have limitations of noise, frequency of operation, power dissipation or dynamic range. For a full discussion see ref(3).

4.1 Hybrid arrays

A particularly attractive infrared detector material is CMT, due to the ability to tailor the bandgap to specific requirements and at the same time fabricate high performance photoconductive or photovoltaic detectors. CMT photovoltaic detectors have been coupled directly to a silicon CCD(7) using direct injection into the CCD. For all direct injection systems using the configuration of fig 4 the input diode with gate and drain electrodes in effect form an MOS transistor. At the low currents obtained in infrared imaging this MOS transistor is in a low-signal regime with $g_m = eI_{SD}/2kT$, giving a marked decline in transfer efficiency at low background fluxes.

An alternative to the wire interconnect used for CMT-Si is the flexible metal interconnect with a 'flip-chip' technology. A number of detector materials have been coupled to silicon readout circuits using this technique, for instance LTT for 8-13μm 1024 detector arrays(8) and a variety of materials for 3-5μm operation, such as InSb(9),(10) and $InAs_xSb_{1-x}$ (11),(12).

The metal interconnect is one problem area, with connection success values of the order of 98% on 1024 elements corresponding to about 20 dead elements. This technology is particularly difficult for LTT which has a large expansion mismatch to silicon, the III-V and II-VI materials have a much better match. The 'flip-chip' approach also favours pseudo binary semiconductors where the photosensitive device layer can be grown on a wider bandgap substrate to give mechanical strength.

An alternative to the 'flip-chip' approach is to use a heterojuction, for instance as described by Steckl[13].

A further alternative that has been extensively reported is the use of an InSb CID array linked to silicon signal processors[14],[3]. This uses 10 24 x 16 InSb CID arrays, which function purely as multiplexers to reduce the number of interconnects, linked to silicon demultiplexers and TDI chips. The InSb CID chips have been extensively described, eg[15] but the silicon processor chips took longer to make than the InSb CID[16].

A pyroelectric detector must be used in the hybrid mode. Although pyroelectric detectors are not as sensitive as photon detectors, as described in section 2 they have a reasonable performance coupled with operation at normal ambient temperatures. A 'flip-chip' technology is indicated, but it is worth remembering that in order to complete with current scanned imager performance of, say D*(500K) = 10^{10}cm $Hz^{\frac{1}{2}}W^{-1}$ on 100 detectors (D* $\sqrt{N}$ = 10^{11} cm $Hz^{\frac{1}{2}}$ W^{-1}) a pyroelectric - CCD combination with a detector D*(500K) of 3.10^{8} cm $Hz^{\frac{1}{2}}$ W^{-1} would require 10^{5} detectors, corresponding to a full staring array.

4.2 Schottky barrier

The application of internal photoemission in a metal-semiconductor Schottky barrier was proposed several years ago[17]. The photon is absorbed in the metal and the hot electron produced can be injected into the semiconductor. The process is a fairly low quantum efficiency (typically 0.1%) with response out to the limit set by the Schottky barrier height for platinum silicide-silicon of 0.27 eV[18] giving a fair match to the 3-5μm waveband. The main advantages are an all silicon technology and a high degree of uniformity. In use the Schottky barrier detector is reset at each read pulse to a reference voltage, and the charge required for this is transferred to the CCD shift register.

In operation the device must be cooled to reduce thermionic emission over the Schottky barrier. Devices reported to date[18],[19] operate around 90K and both line (256 element) and area (25 x 50) arrays have been constructed.

4.3 Monolithic Extrinsic

For focal plane arrays using this technology the only suitable host semiconductor is silicon so that the full power of integrated circuit technology can be exploited. Various authors[20],[21][22],[23] have reviewed the properties of extrinsic silicon as a material, and the main dopants are listed in table 3. Both donors in n-type material and acceptors in p-type material are candidates and in both cases the photo-excitation produces majority carriers. Special CCD input structures are then required to couple the detector to the CCD, an example is shown in fig 5[27]. For thermal imaging the dominant dopants are In (for 3-5μm) and Ga (for 8-13μm) but both suffer from the need for cooling well below 77K for operation with 300K backgrounds. There is currently an active search for dopants capable of operation in the 3-5μm waveband at 77K or above. No dopants have been reported which approach operation in the 8-13μm waveband at this temperature, and it is highly unlikely that conventional dopants will be able to achieve this. The only possibility is that counterdopants, as proposed by Elliott et al[24] may provide a route to this temperature and wavelength regime.

A number of extrinsic silicon arrays have been reported[22],[25],[26]. For this technology it is possible to alter the wavelength of operation by changing the dopant only, keeping the masks and design features unaltered. The largest array reported is a 32 x 96 array[22] with unspecified dopants.

TABLE 3 IMPURITY LEVELS IN SILICON

	ΔE (eV)	λ_{pk} (μm)	$\lambda_{1/2}$ (μm)	$\sigma_{\lambda pk}$ (10^{-16} cm^2)	Solubility (10^{16} cm^{-3})	T_{BLIP} (K)
Donor						
Sb	0.039	28.8	31.5	72	6.8×10^3	-
P	0.044	26.0	29.4	22	1.3×10^5	-
As	0.055	22.5	24.2	15	1.9×10^5	-
Bi	0.070	17.5	18.7	70	80	33
Mg	0.11	11.5	12.1	17	3000	30
Te	0.14	-	8.9	-	>1000	-
S	0.19	5.5	6.8	2	3	72
Yb	0.33	-	-	-	-	-
Tm	0.49	-	-	-	-	-
Acceptors						
B	0.045	23.5	27.8	18	6×10^4	-
Al	0.057-0.069	15	18	4.5-8.5	2×10^3	33
Ga	0.065-0.074	15	17-18	2.6-5.6	3×10^3	33
Be	0.11 -0.15	6	7.4	0.05	-	-
In	0.155	5	7.4	0.33	200	62
Tl	0.23	3.5	4.2	-	>10	-
Ni	0.23	2	3.6-5.4	-	-	-
Cu	0.24	3.75	4.9	0.05	-	86
Te	0.26	3.5	4.2	-	-	-
Zn	0.27-0.3	2.5	3.3	1.4-2	6	110
		3.0	3.7			

DATA FROM REVIEWS BY SCLAR, NELSON, ELLIOTT

4.4 Monolithic Intrinsic

In this technology conventional intrinsic detector materials are used and the logic circuits must now be fabricated in these materials and not in silicon. The only reason for developing a suitable logic technology in these narrow band gap materials is for infrared detectors, so there is no readily available technological base to exploit. Even in the case of

silicon it is only a short time since large arrays of photodetectors numbered only 100's of elements, although now full TV is possible it represents the extreme limit of our available technology.

Three materials have been seriously considered for monolithic intrinsic devices, InSb, LTT and CMT. InSb is suitable only for 3-5μm operation while LTT and CMT are candidates for both 3-5μm and 8-13μm wavebands. LTT is unsuitable for further development using CCD or CID technology due to its very high dielectric constant (approximately 400) with the attendant requirement for an insulator of similar dielectric constant. CCD and CID devices have been reported on InSb, and CCD devices in CMT.

InSb CID detectors have been developed at GE[15] primarily for the hybrid system described in section 4.1[3], but of course the 16 x 24 array would work in its own right as an X-Y addressed CID InSb detector. InSb CCD arrays have been developed at SBRC[28], with a planar technology for the detector and the CCD.

The CCD is 4 phase, surface channel, overlapping gate with the detectors connected to an opaqued CCD shift register by a transfer gate. Full operation of 20 element linear arrays has been achieved with current charge transfer efficiencies of the order of 0.995 at 77K. Predicted performance when a number of improvements are implemented is a D* of 10^{12}cm $Hz^{\frac{1}{2}}$ W^{-1} for backgrounds below 10^{14} photons cm^{-2} sec^{-1}.

The development of CMT CCD devices is more recent, but progress by the group at Texas Instruments[29],[30] has been rapid in material with a bandgap suitable for 3-5μm imaging. Both 16 and 32 bit CCD shift registers have been operated at 77K with transfer efficiencies up to 0.9995 using the four phase structure based on a ZnS insulator on the native oxide shown in fig 6. The n-type CMT was produced by solid state recrystallization with a bandgap of 0.295 to 0.315 eV and a doping level of $1\text{-}2.10^{15}$ cm^{-3}. High D* values have already been obtained, for a 16-stage shift register with 20^{o} field of view, 50 kHz clock and a cutoff wavelength of 4.3μm, a $D^*_{\lambda p}$ of $2.8\ 10^{12}$cm $Hz^{\frac{1}{2}}$ W^{-1} was measured, compared with 4.10^{12} cm $Hz^{\frac{1}{2}}$ W^{-1} for an ideal 16 element TDI detector with the same quantum efficiency (46%).

5 CONCLUSIONS

While single element technology can now provide detectors, and limited size detector arrays, with near-theoretical performance over a wide range of wavelengths, incident photon fluxes and operating temperatures, this is not yet true for higher technology devices incorporating multiplexing or TDI functions. This is apparent in the wide range of materials and technologies currently being studied. Significant progress is being made, however, with most success in devices for 3-5μm 77K operation (eg InSb and CMT monolithic, Si Schottky barrier) and in 3-5 and 8-13μm sub 77K (extrinsic silicon). Hybrid technology requires a solution to the interconnection problem to proceed far beyond the 100 to 1000 element size, but can offer 8-13μm 77K operation.

REFERENCES

1 R Longshore, P Raimondi, M Lumpkin, IR Physics, Vol 16, p 639,1976.

2 D Long, Chapter 4 in 'Topics in Applied Physics', Vol 19, Springer-Verlag, 1977.

3 A F Milton, Chapter 6 in 'Topics in Applied Physics', Vol 19, Springer-Verlag, 1977.

4 eg International Defense Review, p 997, 1976.

5 D E Charlton, M D Jenner, I M Baker, IEE Conference on Low Light and Thermal Imaging, Nottingham 1979, p 37.

6 Plessey Ltd, private communication.

7 S Iwasa, Opt. Eng., Vol 16, p 233, 1977.

8 J M Tracy, A M Andrews, C C Wang, M Ewbank, J T Longo, Device Research Conference, Ithaca NY, 1977, p 6.

9 R M Hoendervoogt, K A Kormos, J P Rosbeck, J R Thoman, C B Burgett, IEDM, Washington 1978, p 510.

10 W J Parrish, F J Renda, N L Ray, D G Maeling, R E Eck, J R Thoman, IEDM, Washington 1978, p 513.

11 J D Blackwell, J P Rode, A M Andrews, G M Williams, W E Tennant, Device Research Conference, Santa Barbara Ca, 1978.

12 A M Andrews, IEDM, Wahsington 1978, p 505.

13 A J Steckl, M E Motamedi, S P Shen, H Elabd, K Y Tam, CCD 78, San Diego, 1978, p 2-39.

14 A Fenner Milton, M Hess, CCD 75 San Diego 1975, p 71.

15 J C Kim, W E Davern, D Colangelo, IEDM, Washington, 1976, p 550.

16 R J Kansy, W F Stephens, D D Buss, T F Cheek, CCD 78, San Diego, 1978, p 2-61.

17 F D Shepherd, A C Yang, IEDM Tech. Digest 1973, p 310.

18 W F Kosonocky, E S Kohn, F V Shallcross, D J Sauer, CCD 78, San Diego, 1978, p 2-27.

19 E S Kohn, IEEE J. Sol. st. Cts, Vol SC-11, No 1, Feb 76, p 139,

20 N Sclar, IR Phys. Vol 16, 1976, p 435.

21 N Sclar, IR Phys. Vol 17, 1977, p 71.

22 R D Nelson, Optical Engineering, Vol 16, No 3, 1977, p 275.

23 B R Holeman, 2nd Int. Conf. on IR Phys., Zurich, 1979, p 158.

24 C T Elliott, P Migliorato, A W Vere, IR Phys. Vol 18, p 65, 1978.

25 K Nummedal, J C Fraser, S C Su, R Baron, R M Finnila, CCD 75 San Diego, 1975, p 19.

26 N Sclar, R L Maddox, R A Florence, App. Optics, Vol 16, p 1525, 1977.

27 D F Barbe, Electro-Optics Systems Design, April 1977, p 50.

28 R D Thom, T L Koch, W J Parrish, AIAA/NASA Conference on Smart Sensors, Hampton Va, 1978.

29 R A Chapman, M S Kinch, S R Borrello, A Simmons, C G Roberts, D D Buss, AIAA/NASA Conference on Smart Sensors, Hampton Va, 1978.

30 D D Buss, R A Chapman, M A Kinch, S R Borello, A Simmons, C G Roberts, IEDM, Washington, 1978.

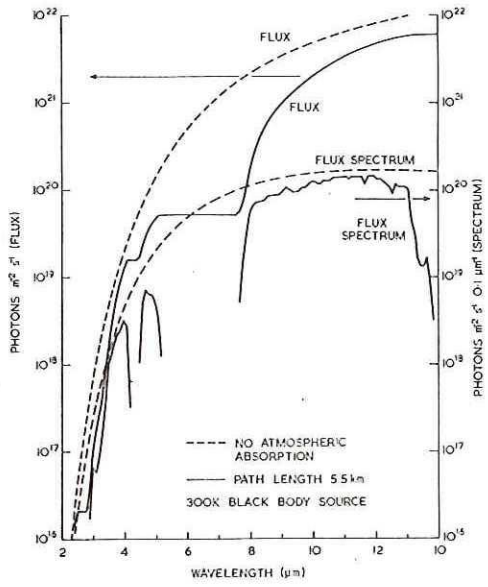

FIG 1 300K RADIATION FLUX SPECTRUM AND INTEGRATED FLUX AS A FUNCTION OF THE LONG WAVELENGTH INTEGRATION LIMIT

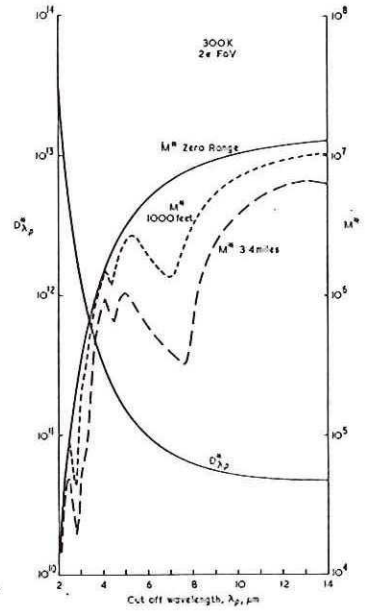

FIG 2 $D^*_{\lambda p}$ AND M^* VERSUS CUT OFF WAVELENGTH λ_p FOR AN IDEAL PHOTON DETECTOR

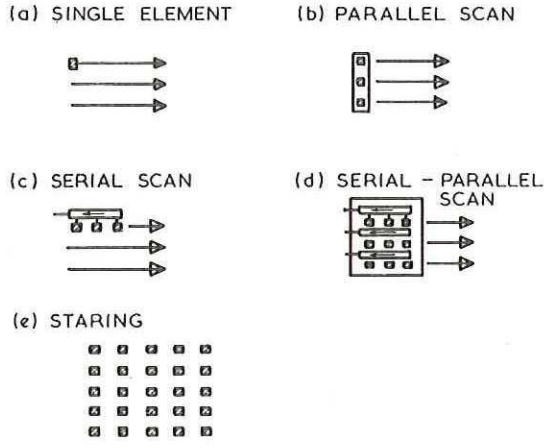

FIG. 3. IMAGER CONFIGURATIONS

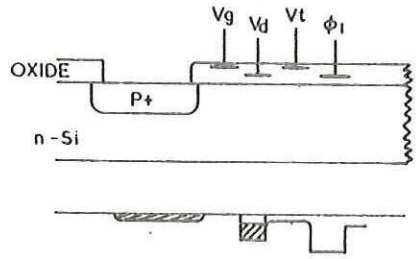

FIG. 4. CONFIGURATION FOR DIRECT INJECTION INTO A CCD

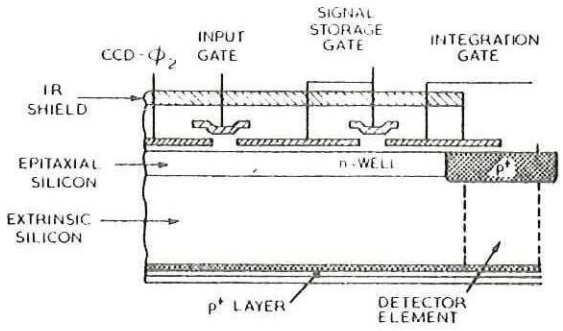

FIG 5 SCHEMATIC DIAGRAM SHOWING A CELL OF AN EXTRINSIC SILICON CCD ARRAY
After Barbe (27)

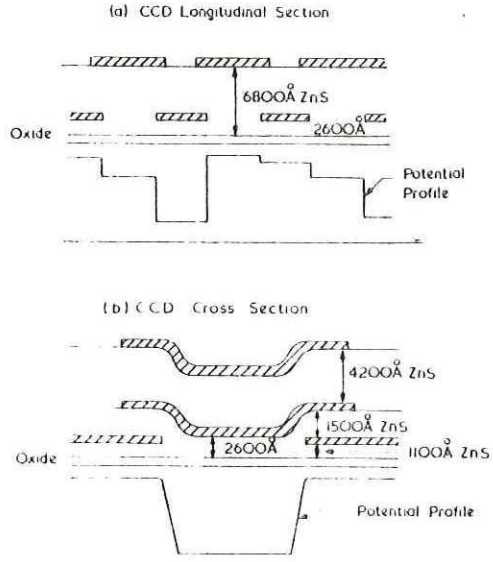

FIG 6 CMT CCD STRUCTURE
After Chapman et al (29)